ADVANCED FUNCTIONAL MATERIALS
www.afm-journal.de

Polymer Grafting by Inkjet Printing: A Direct Chemical Writing Toolset

*Alexandre Garcia, Nassim Hanifi, Bruno Jousselme, Pascale Jégou, Serge Palacin, Pascal Viel, and Thomas Berthelot**

Among all the patterning techniques, inkjet printing has lately become a reliable technique at micrometer scale to produce localized modifications on material surfaces. Printing of polymer on material surface however leads to adsorbed patterns with poor adhesion. To overcome this drawback, a new process combining for the first time inkjet printing and an efficient covalent polymer grafting method was developed. This latter method is based on a photo-assisted reduction of aryldiazonium salt/acrylate monomer ink, derived from the already published GraftFast process. In order to demonstrate its versatility, this new localized polymer grafting process is here combined as an example with the ligand induced electroless plating (LIEP) process to obtain metal interconnects onto flexible and transparent substrates with excellent mechanical and electrical properties for applications in flexible electronics devices.

1. Introduction

Localized modifications of material surfaces have grown in interest over the past three decades and are now used in many industries such as automotive, biotechnology, aerospace, or electronics. Among all the patterning techniques, inkjet printing is the most competitive method at micrometric scale especially for the development of flexible electronics applications. Indeed, inkjet printing is a digitally driven mask-less and one-step process that allows localized deposition on demand with low waste production and at lower cost[1–5] than most of the patterning techniques such as photolithography[5] or other printing techniques such as microcontact printing[7–11] or screen printing.[9,12] However, inkjet printing relies on precursor inks that should generally be annealed after printing in order to provide the expected conducting properties. That annealing step is power-consuming and in many cases incompatible with the polymer substrate. More recently, it has been demonstrated that low or room temperature sintering of nanoparticle inks can be obtained by i) formulating ink with very low molar mass organic additives or ii) using microwave radiations or chemical neutralization of the stabilizer to destruct or discard the organic layer of metallic nanoparticles, or iii) using reactive inkjet printing.[13,5] Those methods look quite promising, but they appear to be quite difficult to print, and the final printed metals exhibit low conductivity compared to bulk metal values.[13,14] Inkjet printing may also be used to pattern catalytic metallic particles for further electroless deposition of thick metal features.[15] In that case, the final mechanical adhesion between the metal features and the polymer strongly depends on the pristine surface properties of the polymer and generally require some surface treatment before printing.[16]

We have recently developed a wet chemical technology based on diazonium salts chemistry, called GraftFast, which provides covalently grafted polymer films exhibiting excellent adhesion and good mechanical properties.[17–23] GraftFast has already been applied to heavy metal waste treatment,[19] chemical biosensing[20] carbon nanotube immobilization[24] and for the electroless plating of polymers.[21,22] However, a direct use of the GraftFast technology with DOD (droplet on demand) inkjet printing is inconsistent for several reasons: i) the cartridge solution must be stable for long storage times, which is difficult with diazonium salts in solution ii) due to the high reactivity of the GraftFast chemistry, the solution must be activated only after deposition on the substrate to prevent the nozzles clogging, which implies a second chemical step after printing and extensive post-reduction rinsing and iii) the droplet, acting as a pL (picoliter) reactor, is incompatible with the GraftFast reaction. Indeed, dioxygen inhibits the GraftFast process by scavenging the formed radicals[25] and each printed "microdroplet" (1.5 pL) can be considered as a "single microreactor" very quickly saturated with oxygen through simple diffusion.

To overcome these drawbacks, which are detrimental to directly combining GraftFast with an inkjet printing technology, we present here an innovative process based on a photo-assisted radical polymerization of a vinylic monomer inside a picoliter droplet that leads to localized covalent polymer grafting. To the best of our knowledge, photo-initiation was never used for surface functionalization involving diazonium salts. Thanks to that innovation, stable printing solutions can be stored within the inkjet cartridges, and the initiation step can easily performed after printing through a simple light irradiation.

Dr. A. Garcia, N. Hanifi, Dr. B. Jousselme, P. Jégou, Dr. S. Palacin, Dr. P. Viel, Dr. T. Berthelot
SPCSI Chemistry of Surfaces and Interfaces Group
CEA, IRAMIS, Gif-Sur-Yvette, 91191, France
E-mail: thomas.berthelot@cea.fr

DOI: 10.1002/adfm.201203544

2. Results and Discussion

2.1. Ink-Jet Polymer Grafting

Usually, photo-induced surface grafting with vinylic or acrylate monomers is mediated by a photo-initiator such as benzophenone.[28] Two main strategies are commonly used: i) the photo-initiator is physically incorporated (by a diffusion process) in the polymer matrix[29] or ii) the photo-initiator is first grafted on the polymer surface.[30] Both approaches could be combined with conventional photolithographic methods to provide *via* multi-step processes polymer patterns on a wide variety of materials materials.[31] We will demonstrate here that these multi-step processes can be replaced by a direct photo-assisted GraftFast technology with DOD inkjet printing.

The localized photo-assisted grafting was carried out with a commercial inkjet printer and an aqueous ink containing an aryldiazonium salt, a vinylic monomer (acrylic acid (AA) as an example), a ruthenium dye $[Ru(bpy)_3]Cl_2$ as a photosensitizer and triethylamine as sacrificial donor. A thickener (namely polyacrylic acid-*co*-maleic acid (PAA-*co*-PMA) selected for its chemical similarity with PAA) was added to the solution to increase its viscosity and improve the inkjet solution wettability onto the substrate and the overall printing resolution. That printing ink showed perfect stability over a full day, and was not tested on longer times. After the printing step, the substrates were exposed to light in the visible range for 1 min. Indeed, the absorbance spectrum of the resulting ink (**Figure 1**) clearly shows a visible absorption (400 to 500 nm) attributed to the metal-ligand charge transfer (MLCT) band of the ruthenium complex,[34] while the other components absorb only in a UV range.

Three types of substrates were selectively printed: gold (used for infrared spectroscopy (IF) and X-ray photoelectron spectroscopy (XPS) characterizations) and two insulating and flexible substrates: poly(ethylene terephtalate) (PET) and polyvinylchloride (PVC) sheets commonly used as transparent substrates for flexible electronics and glossy paper substrates for inkjet or laser printing, respectively.

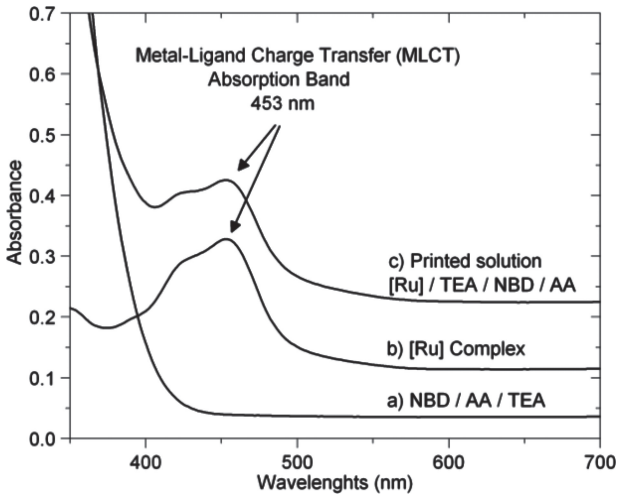

Figure 1. Absorbance of aqueous solutions of a) NBD salt + AA + TEA, b) the (Ru) complex alone and c) the printed solution containing all the components. No absorption at 700 nm was observed for the three solutions; Curves b and c were shifted upwards for clarity.

2.2. Characterization of Ink-Jet PAA Grafting

First, ink-jet PAA grafting was confirmed by Fourier transform infrared spectroscopy–attenuated total reflectance (FTIR-ATR) on gold substrates after rinsing treatments under sonication. To avoid interferences with grafted PAA signals, those FTIR-ATR and XPS characterizations were carried out without any PAA-*co*-PMA thickener in the inkjet solution. Four main peaks at 1725, 1586, 1522, and 1350 cm^{-1} in the IR spectrum after light-induced PAA grafting (**Figure 2**A) can be respectively attributed to the stretching vibrations of COOH and COO- groups from PAA,[26] and nitrophenyl groups (two signals stretching modes) from NBD derivatives.[18] The formation of grafted PAA films was also demonstrated by XPS onto gold surfaces. As illustrated in Figure 2B, a typical C1s core level spectrum is composed of four main peaks. Two peaks centered at 284.4 and 286.8 eV

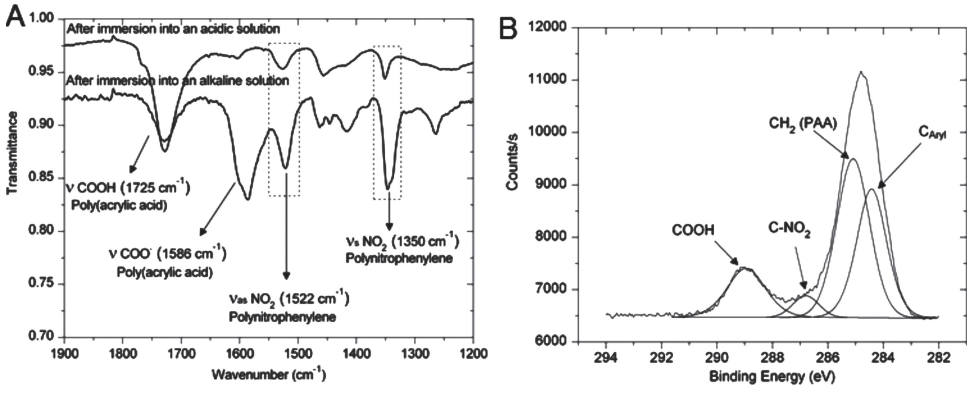

Figure 2. A) IR and B) C1s XPS spectra of gold substrates after photo-assisted PAA grafting.

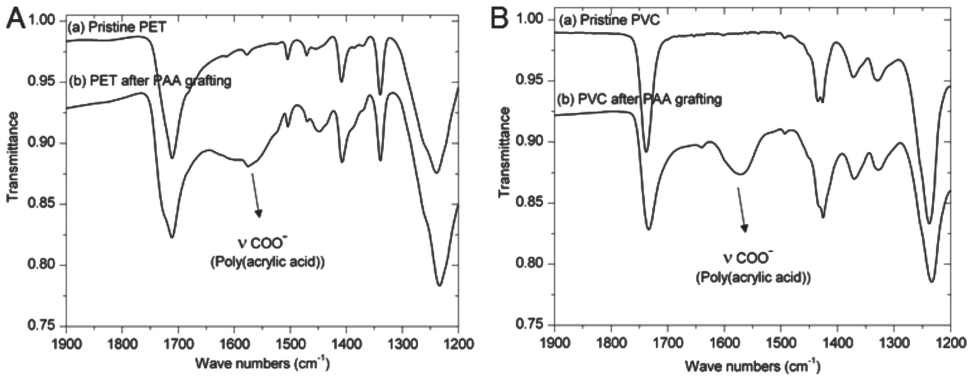

Figure 3. A) IR spectra of pristine PET (a), and the same after photo-assisted PAA grafting (b). B) IR spectra of pristine PVC (a), and the same after ink-jet PAA grafting (b).

respectively correspond to the phenyl carbons C-H and the phenyl carbons bounded to the nitro groups C-NO_2, which confirm the presence of the nitrophenyl groups. Two other peaks centered at 285.2 and 289.0 eV are respectively assigned to CH_2 and COO^- moieties.[39]

Similarly, as shown in **Figures 3**A,B, the IR signature of carboxylic groups appeared after PAA grafting on PET and PVC substrates followed by a harsh rinsing treatment: NaOH 1M at 50 °C for 3 min followed by an immersion for 1 min in deionized water under sonication.[21,22,26] This latter result demonstrates a strong interaction between the grafted PAA chains and the PET and PVC substrates, as already shown for the "classical" GraftFast process.[21,22]

It is worth to mention that: i) the presence of the amine, the diazonium salt, the acrylic monomer and the photosensitizer is critical. Indeed if anyone of these compounds is missing from the inkjet printing solution, no carboxylic functions could be detected on any of the tested substrates, ii) degassing the inkjet printing solution did not change the resulting IR or XPS characterizations, iii) the light-induced grafting process takes only place when the photosensitizer is present and iv) no ruthenium signal could be found in the XPS spectra after rinsing.

2.3. Proposed Mechanism for Ink-Jet Polymer Grafting

In respect to these results and our previous works,[17–23] a complete grafting mechanism, that basically replaces the chemically-induced by a photo-induced reduction of the diazonium salt in our classical GraftFast mechanism, is proposed in **Figure 4**. The ruthenium tris(bipyridine) complex is indeed well known for its electron transfer properties in its excited state, thanks to the MLCT absorption band at 453 nm.[34,37] Thus, under visible irradiation, a photo-induced electron transfer between the ruthenium dye and the aryldiazonium salt induces the formation of an aryl radical (Figure 4a) as previously described.[38,40] The following steps are similar to the ones already proposed for the GraftFast process: covalent grafting of the aromatic radical (Figure 4b), radical polymerization of the acrylic acid initiated by the aromatic radical (Figure 4c) and covalent grafting of the aliphatic chains on the polyphenylene layer (Figure 4d).[17,18,21] Then, the oxidized ruthenium dye is reduced by the excess of triethylamine in the mixture to restart the photo-catalytic process.

Our results show that each printed "microdroplet" (1.5 pL) consists of a "single microreactor" in which the AA radical polymerization actually occurs despite the presence of dioxygen (which is a radical polymerization inhibitor). We consider that the photo-induced initiation, which is very fast, creates almost instantaneously and in the whole volume of the microdroplet a large amount of aryl radicals able to i) react with dissolved oxygen and ii) start the surface functionalization process. Our results demonstrate that the competition between those two pathways is not harmful to the final localized grafting on the

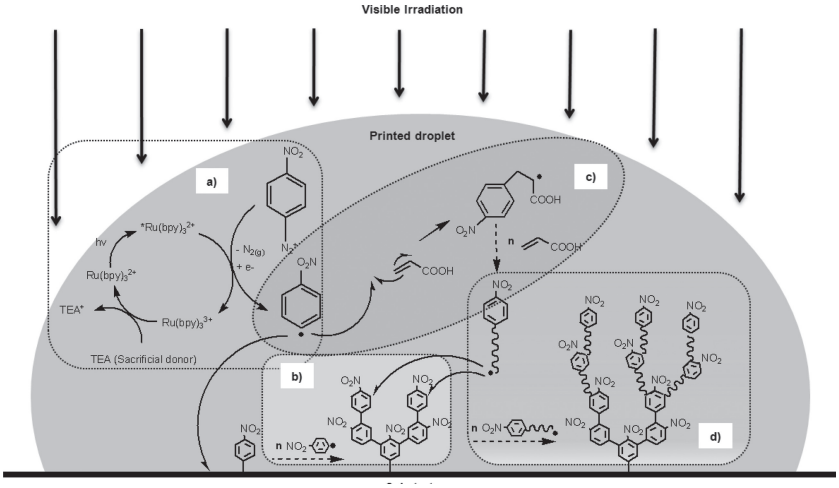

Figure 4. Proposed mechanism divided into four main steps based on the GraftFast process.[17,18] a) Photo-assisted reduction of the aryldiazonium compound (b). Grafting of the resulting aryl radicals onto the surface and growth of the polynitrophenylene multilayer. c) Acrylic acid polymerization initiated by the aryl radicals. d) Polyacrylic acid oligoradicals grafting on the primer layer.

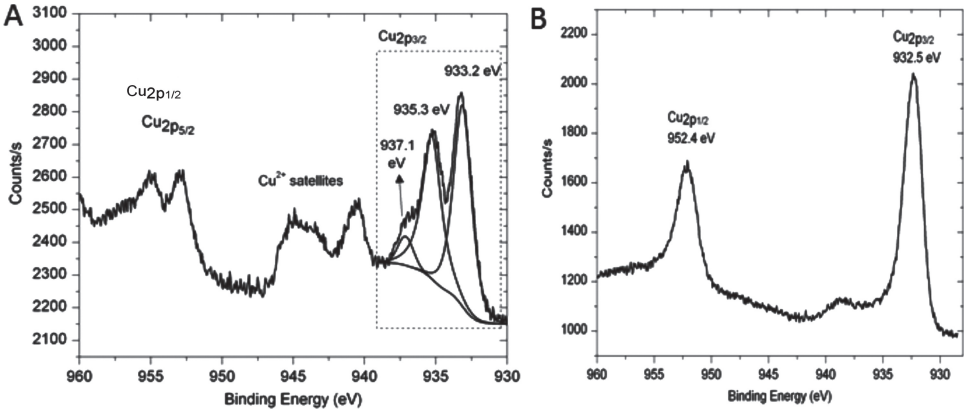

Figure 5. A) Cu_{2p} XPS spectrum after Cu^{2+}-loaded photo-assisted PAA grafting onto PET substrates. B) Cu_{2p} XPS spectrum after Cu reduction onto PET substrates.

surface, which implies that, once the irradiation begins, there is a fast and a complete depletion of the dioxygen concentration contained in the "microreactor". Then, before the oxygen concentration rises again by spontaneous diffusion, the acrylic acid polymerization proceeds following the mechanism described in Figure 4.

Thus, this innovative, versatile and one-step method can be performed in ambient conditions to provide a robust, selective and VOC (volatile organic compound)-free patterning of the substrate properties.

2.4. Metallization of Ink-Jet Grafted Patterns

We then decided to combine this photo-assisted inkjet process with the ligand induced electroless plating (LIEP) process[21,22,26] for the easy fabrication of copper patterns on polymer substrates. Metal interconnect fabrication onto polymer substrates by inkjet printing has been thoroughly investigated, but mostly requires a sintering step above 150 °C, in order to improve the conducting properties of the printed metal patterns based on pristine metal particles.[1,32,33] That is the main bottleneck of inkjet printing on polymers since the glass transition temperature of commonly used polymers, like poly(ethylene terephtalate) (PET) or polycarbonate (PC), is below 150 °C.

By adding copper sulfate ($CuSO_4$, $5H_2O$) to the previously described inkjet solution and thanks to the chemical properties of the carboxylic groups in PAA, a thin Cu^{2+}-loaded and covalently grafted poly(acrylic acid) (PAA) film was obtained after 1 min of visible light irradiation. Cu^{2+}-loaded PAA grafting was confirmed by FTIR-ATR and XPS analysis. Hence, photo-induced PAA grafting did not seem to be disturbed by the presence of Cu^{2+} ions which are not concerned by the photoreduction process, as indicated by XPS analysis (**Figure 5**A).[35] The Cu_{2p} spectra analysis confirmed the Cu^{2+} chelation by three main peaks respectively corresponding to $Cu_{2p3/2}$ (933.2, 935.3, and 937.1 eV), Cu_{2p} satellites (from 938 to 947 eV) and $Cu_{2p1/2}$ (953.2 and 954.8 eV) core level binding energies.[39] The different peaks observed for $Cu_{2p3/2}$ and $Cu_{2p1/2}$ are probably due to different conformations of the PAA or PAA-*co*-PMA chains which induced differences in the Cu environment and its binding energy to the carboxylate groups. No direct electron transfer occurs between the ruthenium tris(bipyridine) complex and Cu^{2+} ions since copper still appears in its Cu^{II} oxidation state within the final PAA grafted film. Cu^{2+}-loaded printed substrates obviously derive from complexation of Cu^{2+} by the carboxylate groups contained all along the grafted PAA chains and the entrapped PAA-*co*-PMA thickener. The main advantage in introducing Cu^{2+} ions directly in the inkjet solution lies in saving process steps and time compared to the common immersion process.[22]

Subsequent reduction of the Cu^{2+} ions provides the catalyst for the electroless metal growth which starts inside the grafted host polymer.[22] Indeed, after immersion into a sodium borohydride solution, the Cu^{2+} reduction into Cu^0 was confirmed by XPS measurements with two main peaks corresponding to $Cu_{2p3/2}$ (932.5 eV) and $Cu_{2p1/2}$ (952.4 eV) core level binding energies (Figure 5B).[39]

The resulting thickness of the catalytic Cu^0-grafted layer was approximately evaluated by mechanical profilometry at ca. 50 nm, which is around six times less than before the borohydride reduction (**Figure 6**c,d). This result validates our decision to avoid any rinsing before the reduction step: the excess of thickener and ungrafted PAA are obviously discarded by an alkaline solution, even after the reduction of the cupric ions.

Finally, the obtained metallic layers were characterized after the Cu electroless plating step catalyzed by that Cu^0-grafted layer.[36]

Figure 6 illustrates the whole process on the example of a copper RFID coil onto flexible and transparent PET. Optical images of Cu^{2+}/PAA-grafted PET are given before and after the electroless copper plating (Figure 6a,c and Figure 6b,d, respectively). They illustrate the process conformity at the micrometric scale since electroless plated copper is present only on the grafted-PAA pattern. As a matter of fact, the local Cu^{2+}/PAA coating can be considered as a latent image which is then developed when the entire substrate is introduced into the electroless plating bath. Additionally, as shown in Figure 6g, the 1-µm-thick plated-copper pattern showed quite homogeneous and uniform in thickness as analyzed by mechanical profilometry.

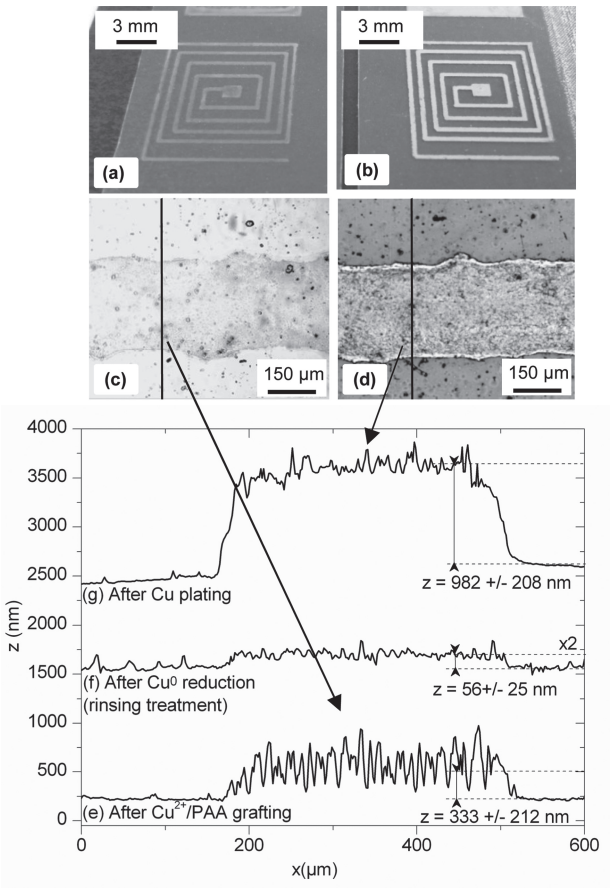

Figure 6. a,b) Optical images of Cu^{2+}/PAA-patterned PET sheets and b,d) the corresponding Cu-patterned PET sheets at different scales and the profile extracted at each step: e) after Cu^{2+}/PAA grafting, f) after Cu reduction, and g) Cu plating.

Other examples of copper patterns obtained on PET and PVC sheets are given in **Figures 7**A,B. They all illustrate that the final resolution is not controlled by the chemistry of the process but by the printer itself, which is a clear asset of our process. For the present work, we have been using a commercial printer that produces droplets of 1.5 pL. More expensive professional head-inkjet printers do not form smaller droplets, but are able to print larger surfaces much faster. Hence, the resolution cannot be improved if professional head-inkjet printers is used. Our process is by the way fully compatible with classical photo- or electrolithography, where a temporary mask can be deposited on the surface to prevent designated areas to be functionalized by the light-induced polymer grafting process. In that case, the final resolution can be significantly increased, at the cost of the whole process.

The adhesion of the plated copper films was checked with the classical cross-cut tape test. For both 1-µm-thick copper plated PET and PVC substrates, none of the cross-hatched squares was removed. Such as in the case of our previous works,[21,22] these excellent adhesion results can be attributed to the mechanical interlocking effect between the copper metal film and the photografted polymer, which mimics the micron-scale interdigitation that occurs between the metal layer and the rough interface that results from the toxic chromic acid treatment commonly used in the electroplating industry.

2.5. Electrical Properties Measurements on Flexible Sheets

The resistivity of copper interconnects (Figure 7B and **Figure 8**) photo-grafted onto PET and PVC substrates was measured at 3.0 µΩ cm without any mechanical stress, i.e., within the range classically observed on electroless copper surfaces (2–3 µΩ cm). This value corresponds to a conductivity of 100% of bulk copper. Electrical properties of the copper tracks were also studied under mechanical stress by measuring the electrical resistivity while bending the polymer sheets around cylinders with two radii of curvature equal to 5 and 1.5 mm respectively. The copper interconnects were submitted to 150 cycles of repetitive strain around the cylinders (100 cycles with the 5 mm-radius cylinder, followed by 50 cycles with the 1.5-mm cylinder).

As shown in Figure 8, 100 cycles of repetitive strain around the 5-mm-radius cylinder induced an increase in metal resistivity from 3 to 6 µΩ cm which corresponds to a conductivity of 50% of bulk copper. A more important resistivity increase was however observed when 50 cycles around the 1.5-mm-radius cylinder were added to the previous deformations. Then, the resulting conductivity was 24% of bulk copper. The ability of our copper interconnects on flexible PET foils to tolerate tensile strain was attributed to the strong adhesion between the copper wire and the substrates as previously described for the LIEP process on full substrates.[21,22]

3. Conclusion

In summary, we present a robust and almost waste-free polymer patterning process suitable for a large range of substrates by direct covalent grafting of PAA by inkjet printing. This visible

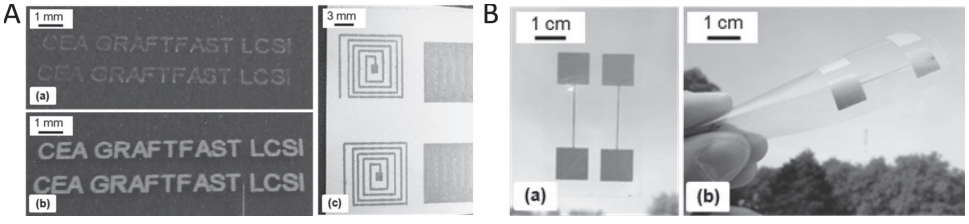

Figure 7. A) Pictures of after PAA-patterned PET sheets (a) and the corresponding Cu-patterned PET sheets (b) and Cu-patterned PVC sheets (c). B) Pictures of Cu-patterned PET sheets used for resistivity measurements.

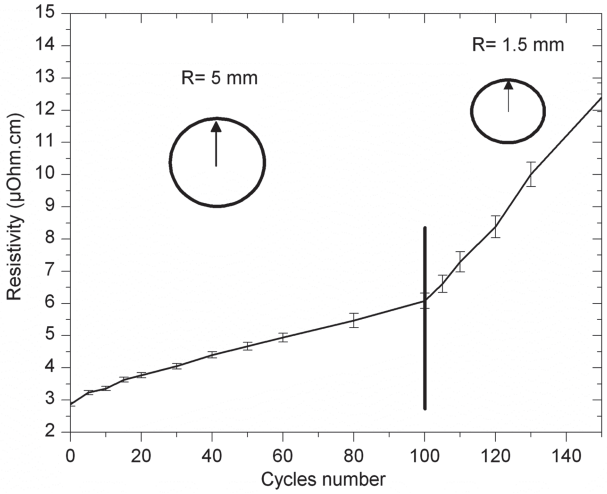

Figure 8. Resistivity measurements of Cu wires grafted on PET sheets and submitted to 100 cycles of repetitive strain around a cylinder with radius with the 5-mm-radius cylinder, followed by 50 cycles with the 1.5-mm-radius cylinder.

light-induced process was demonstrated on gold, PET and PVC substrates. This process combined with the PAA-based LIEP process was also used for the fabrication of micrometric metal patterns with excellent adhesion results of the metal layer onto the substrate and very promising electrical properties. Lastly, in the near future, this process will be extended to various dyes absorbing at different wave numbers, to other substrates, and to another acrylate or vinylic monomers in order to extend the conceivable academic and industrial applications fields of this polymer grafting inkjet-printed process.

4. Experimental Section

Photo-Assisted Polymer Covalent Grafting by Inkjet Printing: Inkjet printing was carried out with a commercial inkjet printer (EPSON Stylus P50) equipped with a piezoelectric drop-on-demand technology (Epson Micro Piezo) using an 5760 × 1440 optimized dpi resolution (≈3.5 μm) and a minimum ink droplet size about 1.5 pL on three different types of substrates: flexible (100-μm-thick) poly(ethylene terephtalate) (PET) sheets of technical quality obtained from Tektronix as standard transparency films, flexible (500-μm-thick) polyvinylchloride (PVC) papers of technical quality from MGI SA (France) and gold substrates made by successive metallic evaporation of chromium underlayer (5 nm) and gold as top coat (200 nm) on microscopic glass slides (BALZERS BAK600). The inkjet solutions were always made first by mixing the 4-nitrobenzenediazonium tetrafluoroborate (200 mg) to aqueous solutions of $[Ru(bypy)_3]Cl_2$ (4 mL, 5.10^{-4} M) and triethylamine (2 mL, 0.1 M). Then, acrylic acid (2 mL) and polyacrylic acid-*co*-maleic acid sodium salt (200 mg, average M_w = 50 000 g mol^{-1}) were added to the previous solution. After printing at room temperature (20 °C, 40% humidity), the patterned surfaces were irradiated through a visible halogen desk lamp (OSRAM, 100 W) for 1 min. The major part of the emitted energy (up to 85%) lies in the infrared and near-infrared regions of the spectrum, 15–20% in the visible range (400 to 700 nm), and less than 1% in the ultraviolet range (below 400 nm). Some experiments were carried out using a UV filter on pipette-deposited droplets, in order to assess the actual role of UV light on the photo-assisted grafting: no differences were observed with respect to filter-free irradiations.

The grafted substrates were then immersed for 3 min in alkaline solution (1 M NaOH, which is the best solvent for ungrafted PAA polymer) at 50 °C and then sonicated for 1 min in deionized water. That treatment was shown by IR analysis sufficient to discard most of the physisorbed matter and equivalent to our usual surface treatment.[21,22,26]

Ligand Induced Electroless Plating: In order to obtain metal patterns based on the LIEP process on polymers substrates, copper sulfate ($CuSO_4$, $5H_2O$, 100 mg) was added to the inkjet solution and allowed to obtain Cu^{2+}-loaded PAA grafting after irradiation, following the same procedure described above for Cu-free mixtures, except for the rinsing step. Indeed, as the reduction step (see below) was performed in alkaline conditions, no rinsing was done before the reduction in order to simplify the procedure. The Cu^{2+} ions chelated by the carboxylate groups contained in the grafted PAA films were then reduced through the substrate immersion into a sodium borohydride ($NaBH_4$) (0.1M)–NaOH (0.1 M) solution at 50 °C for 3 min followed by a rinsing treatment in deionized water. Finally, the patterned surface-activated substrates were placed in an industrial electroless copper plating bath (M Copper 85) using formaldehyde (HCHO) as the reducing agent, and optimum conditions were: copper content 2 g L^{-1}, HCHO/Cu mass ratio = 2, pH 13, working temperature 48 °C to get a deposition rate of ca. 4 μm h^{-1}. The polymer substrates were left in the bath for 30 min.

Spectroscopic Methods: Infrared spectra were recorded on a Bruker Vertex 70 spectrometer equipped with an Attenuated Total Reflection (ATR) Pike-Miracle accessory. The detector was a MCT working at liquid nitrogen temperature. The spectra were obtained after 256 scans at 2 cm^{-1} resolution.

XPS studies were performed with a KRATOS Axis Ultra DLD spectrometer, using the monochromatized Al Kα line at 1486.6 eV. The pass energy of the analyzer was kept constant at 20 eV for C1s core level scans. The photoelectron take-off angle was 90° with respect to the sample plane, which provides an integrated sampling probe depth range going from 7 to 20 nm for the substrates.

Mechanical Adhesion Test: The adhesion between the metallic layer and the polymer sheets was studied by the standard ASTM D3359 Scotch tape test (cross-cut tape test) which consists in applying and removing pressure-sensitive adhesive tape over 16 cross-hatched squares of 1 mm × 1 mm made in the film by an Elcometer Cross Hatch cutter (Elcometer 107 X-Hatch ASTM Kit). That well-used test allows direct comparison of the adhesion of films obtained under various conditions on similar substrates.

Electrical Properties: Electrical properties were measured on tracks with the following dimensions: length = 2 cm, width = 300 μm and height = 500 nm measured by profilometry, and terminal pads of 1 cm^2 for electrical contact. The resistivity of the wire was measured thanks to a four-point probe set-up using a home-built constant current source as described in Keithley's handbook.[27]

Received: November 30, 2012
Revised: January 3, 2013
Published online: February 19, 2013

[1] J. Perelaer, C. E. Hendriks, C. E. de Laat, U. S. Schubert, *Nanotechnology* **2009**, *20*, 165303.
[2] M. Singh, H. M. Haverinen, P. Dhagat, G. E. Jabbour, *Adv. Mater.* **2010**, *22*, 673.
[3] J. W. Song, J. Kim, Y. H. Yoon, B. S. Choi, J. H. Kim, C. S. Han, *Nanotechnology* **2008**, *19*, 095702.
[4] T. H. J. van Osch, J. Perelaer, A. W. M. de Laat, U. S. Schubert, *Adv. Mater.* **2008**, *20*, 343.
[5] P. J. Smith, A. Morrin, *J. Mater. Chem.* **2012**, *22*, 10965.
[6] B. D. Gates, Q. B. Xu, M. Stewart, D. Ryan, C. G. Willson, G. M. Whitesides, *Chem. Rev.* **2005**, *105*, 1171.
[7] D. Aldakov, Y. Bonnassieux, B. Geffroy, S. Palacin, *ACS Appl. Mater. Interfaces* **2009**, *1*, 584.

[8] M. S. Miller, H. L. Filiatrault, G. J. E. Davidson, M. Luo, T. B. Carmichael, *J. Am. Chem. Soc.* **2010**, *132*, 765.
[9] D. Qin, Y. N. Xia, G. M. Whitesides, *Nat. Protoc.* **2010**, *5*, 491.
[10] E. C. Hagberg, J. C. Scott, J. A. Shaw, T. A. von Werne, J. A. Maegerlein, K. R. Carter, *Small* **2007**, *3*, 1703.
[11] O. Azzaroni, Z. Zheng, Z. Yang, T. S. Huck, *Langmuir* **2006**, *22*, 6730.
[12] F. C. Krebs, *Sol. Energy Mater. Sol. Cells* **2009**, *93*, 394.
[13] J. Perelaer, P. J. Smith, D. Mager, D. Soltman, S. K. Volkman, V. Subramanian, J. G. Korvinkdf, U. S. Schubert, *J. Mater. Chem.* **2010**, *20*, 8446.
[14] M. Grouchko, A. Kamyshny, D.-F. Anghel, C. F. Mihailescu, S. Magdassi, *ACS Nano* **2011** *5*, 3354.
[15] W. D. Chen, Y. H. Lin, C. P. Chang, Y. Sung, Y. M. Liu, M. D. Ger, *Surf. Coat. Technol.* **2011**, *205*, 4750.
[16] S. Jang, H. Cho, S. Kang, S. Oh, D. Kim, *Appl. Phys. A* **2011**, *105*, 685.
[17] V. Mevellec, S. Roussel, L. Tessier, J. Chancolon, M. Mayne-L'Hermite, G. Deniau, P. Viel, S. Palacin, *Chem. Mater.* **2007**, *19*, 6323.
[18] A. Mesnage, S. Esnouf, P. Jegou, G. Deniau, S. Palacin, *Chem. Mater.* **2010**, *22*, 6229.
[19] X. T. Le, P. Viel, A. Sorin, P. Jegou, S. Palacin, *Electrochim. Acta* **2009**, *54*, 6089.
[20] T. Berthelot, A. Garcia, X. T. Le, J. El Morsli, P. Jegou, S. Palacin, P. Viel, *Appl. Surf. Sci.* **2011**, *257*, 3538.
[21] A. Garcia, T. Berthelot, P. Viel, J. Polesel-Maris, S. Palacin, *ACS Appl. Mater. Interfaces* **2010**, *2*, 3043.
[22] A. Garcia, J. Polesel-Maris, P. Viel, S. Palacin, T. Berthelot, *Adv. Funct. Mater.* **2011**, *21*, 2096.
[23] V. Mévellec, S. Roussel, D. Deniau, *World Patent, WO2008078052*, **2006**.
[24] P. Viel, X. T. Le, V. Huc, J. Bar, A. Benedetto, A. Le Goff, A. Filoramo, D. Alamarguy, S. Noel, L. Baraton, S. Palacin, *J. Mater. Chem.* **2008**, *18*, 5913.
[25] J. Brandrup, E. H. Immergut, E. A. Grulke, A. Abe, D. R. Bloch, *Polymer Handbook*, 4th Ed., John Wiley & Sons, Chichester **2005**.
[26] A. Garcia, T. Berthelot, P. Viel, A. Mesnage, P. Jegou, F. Nekelson, S. Roussel, S. Palacin, *ACS Appl. Mater. Interfaces* **2010**, *2*, 1177.
[27] *Low Level Measurements Handbook*, Keithley Instruments, Cleveland **2007**.
[28] R. C. Advincula, W. J. Brittain, K. C. Caster, J. Ruhe, *Polymer Brushes. Synthesis, Characterization, Applications,* Wiley-VCH Verlag, Weinheim **2004**
[29] M. H. Schneider, Y. Tran, P. Tabeling, *Langmuir* **2011**, *27*, 1232.
[30] J. Mosnáček, I. Lukáč, M. Bertoldo, F. Ciardelli, *Chem. Papers* **2013**, *67*, 9.
[31] T. Rohr, D. F. Ogletree, F. Svec, J. M. J. Fréchet, *Adv. Funct. Mater.* **2003**, *13*, 264.
[32] S. Jeong, H. C. Song, W. W. Lee, S. S. Lee, Y. Choi, W. Son, E. D. Kim, C. H. Paik, S. H. Oh, B. H. Ryu, *Langmuir* **2011**, *27*, 3144.
[33] D. Q. Vo, E. W. Shin, J. S. Kim, S. Kim, *Langmuir* **2010**, *26*, 17435.
[34] J. E. Huheey, E. A. Keiter, R. L. Keiter, *Inorganic Chemistry*, De Boeck Université, Bruxelles **1998**.
[35] G. Beamson, D. Briggs, *High Resolution XPS of Organic Polymers: The Scienta ESCA300*, John Wiley & Sons, Chichester **1992**.
[36] G. O. Mallory, J. B. Hajdu, *Electroless plating: Fundamentals and Applications*, The American Electroplaters and Surface Finishers Society, Washington, DC **1990**.
[37] B. Jousselme, G. Bidan, M. Billon, C. Goyer, Y. Kervella, S. Guillerez, E. Abou Hamad, C. Goze-Bac, J. Y. Mevellec, S. Lefrant, *J. Electroanal. Chem.* **2008**, *621*, 277.
[38] W. Horspool, F. Lenci, *CRC Handbook of Organic Photochemistry and Photobiology Second Edition*, CRC Press, Boca Raton **2004**.
[39] G. Beamson, D. Briggs, *High Resolution XPS of Organic Polymers: The Scienta ESCA300*, John Wiley & Sons, Chichester **1992**.
[40] T. Hering, D. Prasad Hari, B. Konig, *J. Org. Chem.* **2012**, *77*, 10347.